Article

On the Origin of Optical Activity in Tris-diamine Complexes of Co(III) and Rh(III): A Simple Model Based on Time-Dependent Density Function Theory

Francisco Elias Jorge, Jochen Autschbach, and Tom Ziegler

J. Am. Chem. Soc., **2005**, 127 (3), 975-985• DOI: 10.1021/ja047670f • Publication Date (Web): 30 December 2004

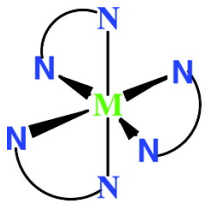

Λ-M(en)$_3^{3+}$

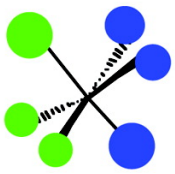

L_σ

Mπ

More About This Article

Additional resources and features associated with this article are available within the HTML version:

- Supporting Information
- Links to the 12 articles that cite this article, as of the time of this article download
- Access to high resolution figures
- Links to articles and content related to this article
- Copyright permission to reproduce figures and/or text from this article

View the Full Text HTML

J|A|C|S
ARTICLES
Published on Web 12/30/2004

On the Origin of Optical Activity in Tris-diamine Complexes of Co(III) and Rh(III): A Simple Model Based on Time-Dependent Density Function Theory

Francisco Elias Jorge,[†,‡] Jochen Autschbach,[†,§] and Tom Ziegler*,[†]

Contribution from the Department of Chemistry, University of Calgary, Calgary, Alberta, Canada, T2N-1N4, Departamento de Fisica, Universidade Federal do Espirito Santo, 29060-900 Vitoria, ES, Brazil, and Department of Chemistry, University at Buffalo, State University of New York, 312 Natural Sciences Complex, Buffalo, New York 14260-3000

Received April 22, 2004; E-mail: ziegler@ucalgary.ca

Abstract: Time-dependent density functional theory (TD-DFT) is applied to the CD spectra of $\Lambda(\delta\delta\delta)$-(+)-$[Co(S\text{-}pn)_n(en)_{3-n}]^{3+}$ ($n = 1, 2, 3$) and $\Lambda(\delta\delta\delta)$-(+)-$[Co(en)_3]^{3+}$ as well as the stereoisomers Δ-$((\delta)_n(\lambda)_{3-n})$-(−)-$[Co(S\text{-}pn)_n(en)_{3-n}]^{3+}$ ($n = 1, 2, 3$) and $\Delta(\delta\delta\delta)$-(−)-$[Co(en)_3]^{3+}$. Theory is able to reproduce the major differences in the CD spectra of the species with a Λ-configuration and their isomers with a Δ-configuration in both the d−d and ligand-to-metal CT region. It is further possible to rationalize the trend in terms of a larger azimuthal distortion away from the octahedral geometry in the Λ-conformation compared to the Δ-configuration. Considerations were also given to the CD spectra of the *lel*$_3$-isomer, $\Delta(\lambda\lambda\lambda)$-(−)-$[Rh(R\text{-}pn)_3]^{3+}$ and the *ob*-isomer, $\Lambda(\lambda\lambda\lambda)$-(+)-$[Rh(S\text{-}pn)_3]^{3+}$.

Introduction

Circular dichroism (CD) of transition metal complexes has been studied experimentally since the pioneering work by Cotton[1a] in 1895. In fact, the presence of metal complexes with the same empirical formula but different optical activities has played a decisive role in understanding the stereochemistry of transition metal complexes. However, despite all the studies optical activity in transition metal complexes is far less well understood than that in organic molecules. The reason for this can be attributed to the fact that transitions in metal complexes are more complex as they involve d−d and ligand-to-ligand transitions as well as metal-to-ligand charge transfer (CT).

Moffit introduced the first quantum mechanical theory of optical activity for d-to-d excitations in transition metal complexes.[1b] His work provided an important stimulus for much of the subsequent theoretical effort in this area. Further, theoretical developments[2−4] have been greatly aided by the very large volume of chiroptical and structured data generated for transition metal complexes. Of special importance in this symbiosis between experiment and theory has been tris-diamine complexes of Co(III). However, despite several attempts, no theory has been able to rationalize in simple terms the configurational and conformational effects observed in CD spectra of Co(III) tris-diamine complexes for both d−d and CT transitions.

Time-dependent density functional theory (TD-DFT)[5−11] has become an important tool for the theoretical treatment of electronic excitation spectra[12−20] and frequency-dependent multipole polarizabilities and related properties[21−23] of molecules.

† University of Calgary.
‡ Universidade Federal do Espirito Santo.
§ University at Buffalo, State University of New York.

(1) (a) Cotton, A. *C. R. Hebd. Seances Acad. Sci.* **1895**, *120*, 989−1044. (b) Moffit, W. *J. Chem. Phys.* **1956**, *25*, 1189−1198. (c) Liehr, A. D. *J. Phys. Chem.* **1964**, *68*, 665−722.
(2) Karipides, A.; Piper, T. S. *J. Chem. Phys.* **1964**, *40*, 674−682.
(3) Mason, S. F.; Seal, R. H. *Mol. Phys.* **1976**, *31*, 755−775.
(4) Moucharafieh, N. C.; Eller, P. G.; Bertrand, J. A.; Royer, D. J. *Inorg. Chem.* **1978**, *17*, 1220−1222.
(5) Salahub, D. R.; Fournier, R.; Manarski; P.; Papai, I.; St-Amant, A.; Ushio, J. *Density Functional Methods in Chemistry*; Labanowski, J.; Andzelm, J., Eds.; Springer, New York, 1991; pp 77−100.
(6) Andzelm, J. *Density Functional Methods in Chemistry*; Labanowski, J.; Andzelm, J., Eds.; Springer, New York, 1991; pp 155−174.
(7) Jones, R. O.; Gunnarson, O. *Rev. Mod. Phys.* **1989**, *61*, 689−746.
(8) Runge, E.; Gross, E. K. U. *Phys. Rev. Lett.* **1984**, *52*, 997−1000.
(9) Gross, E. K. U.; Kohn, W. *Adv. Quantum Chem.* **1990**, *21*, 255−287.
(10) Casida, M. E. Time-dependent density functional response theory for molecules. In *Recent advances in density functional methods*; Chong, D. P., Ed.; World Scientific: Singapore, 1995; Vol. 1, pp 155−192
(11) Gross, E. K. U.; Dobson, J. F.; Petersilka, M. *Top. Curr. Chem.* **1996**, *181*, 81−113.
(12) Bauernschmitt, R.; Ahlrichs, R. *Chem. Phys. Lett.* **1996**, *256*, 454−464.
(13) Jamorski, C.; Casida, M. E.; Salahub, D. R. *J. Chem. Phys.* **1996**, *104*, 5134−5147.
(14) Görling, A.; Heinze, H. H.; Ruzankin, S. P.; Staufer, M.; Rösch, N. *J. Chem. Phys.* **1999**, *110*, 2785−2799.
(15) Hirata, S.; Head-Gordon, M. H. *Chem. Phys. Lett.* **1999**, *302*, 375−382.
(16) Solomon, E. I.; Lever, A. B. P., Eds. *Inorganic Electronic Structure and Spectroscopy*; Wiley: New York, 1999; Vols. 1 and 2.
(17) Rosa, A.; Baerends, E. J.; van Gisbergen, S. J. A.; van Lenthe, E.; Groeneveld, J. A.; Snijders, N. G. *J. Am. Chem. Soc.* **1999**, *121*, 1, 10356−10365.
(18) Ricciardi, G.; Rosa, A.; van Gisbergen, S. J. A.; Baerends, E. J. *J. Phys. Chem. A* **2000**, *104*, 635−643.
(19) van Gisbergen, S. J. A.; Groeneveld, J. A.; Rosa, A.; Snijders, J. G.; Baerends, E. J. *J. Phys. Chem. A* **1999**, *103*, 6835−6844.
(20) Ziegler, T. *J. Chem. Soc., Dalton Trans.* **2002**, 642−652.
(21) Osinga, V. P.; van Gibergen, S. J. A.; Snijders, J. G.; Baerends, E. J. *J. Chem. Phys.* **1997**, *106*, 5091−5101.
(22) van Gibergen, S. J. A.; Snijders, J. G.; Baerends, E. J. *Phys. Rev. Lett.* **1997**, *78*, 3097−3100.
(23) van Gibergen, S. J. A.; Kootstra, F.; Schipper, P. R. T.; Grisenko, O. V.; Snijders, J. G.; Baerends, E. J. *Phys. Rev. A* **1998**, *57*, 2556−2571.

Scheme 1. Lowest Singlet Excited States for an Octahedral Complex with a d^6 Ground-State Configuration and Their Splitting on Reduction of the Symmetry into D_{3d} Point Group Symmetry

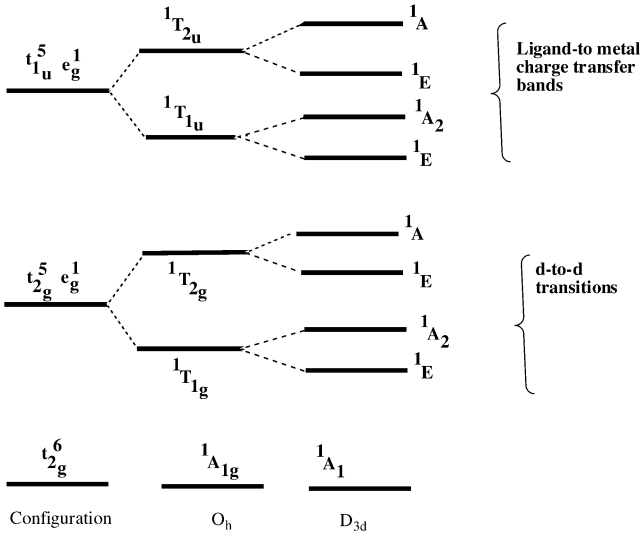

Its success is rooted in a compromise between accuracy and computational efficiency. The theory has a simple, intuitive structure, since it uses the single-particle density as the basic variable in terms of which the total energy can be expressed as a functional. Unfortunately, the exact expression of the energy as a functional of the density is unknown. Thus, in practice one has to resort to approximate relations (functionals).

Recently, electronic and vibrational CD spectra of organic molecules[24,25] as well as of transition metal complexes[26−28] have been investigated by TD-DFT. This theory was also used in initial exploratory studies of the optical activity of tris-bidentate Co(III) and Rh(III) complexes.[26,29a] We shall in the present work take these exploratory studies one step further by providing a simple picture of the configurational and conformational effects observed in CD spectra of Co(III) tris-diamine complexes for both d−d and CT transitions based on qualitative TD-DFT calculations.

The low-energy part for the CD spectra of Co(III) tris-diamine complexes represents HOMO-to-LUMO d-to-d transitions, from t_{2g} to e_g d-based orbitals, Scheme 1. The excitations to $^1E_1$ and $^1A_2$ of $^1T_{1g}$ O_h parentage in the d−d transition CD spectra are the most intense as they are magnetically allowed and able (as we shall see) to borrow electric intensity from the allowed CT transitions, see Scheme 1. At higher energy their recorded spectra consist of ligand-to-metal CT transitions from the t_{1u} ligand orbital to the metal-based LUMO e_g, see Scheme 1. Here the excitations to $^1E_1$ and $^1A_2$ of $^1T_{1u}$ O_h parentage in the CT CD spectrum are the most intense as they are electrically allowed and able (as we shall see) to borrow magnetic intensity from d−d transitions, see Scheme 1.

Scheme 2. Δ- and Λ-Configurations of $Co(en)_3^{3+}$

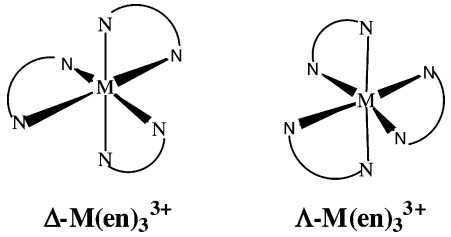

Tris-diamine complexes of Co(III) and Rh(III) exist in the two enantiomeric configurations, Δ or Λ, depending on whether the chelate chains are part of a right-handed or left-handed helix, Scheme 2. In addition the conformation of the rings around the metal are characterized by the distortion of the chelating nitrogens away from the ideal octahedron. We will consider the distortions of the octahedron to consist of an axial (or polar) displacement which will elongate or compress the octahedron along the three-fold C_3 axis, see Scheme 3, and a radial (or azimuthal) distortion consisting of a twist about the three-fold axis, see Scheme 4. In accordance with the nomenclature developed by Stiefel and Brown,[29b] we will use the parameter *s*/*h* (side/height), see Scheme 3, as a measure for the polar displacement and Φ, see Scheme 4, as a parameter for the radial (or azimuthal) distortion. We recall that for an octahedron: *s*/*h* = 1.22 and Φ = 60°.

Corey and Bailar[29c] have shown that ethylenediamine in chelate complexes can adopt one of the two enantiomorphous conformations, λ and δ, in which the N−N direction and the C−C bond define a segment of a left-handed or a right-handed helix, respectively, Scheme 5. For a tris-ethylenedimine complex, if the C−C bond of each chelate ring is approximately parallel to the C_3 axis of the complex, one has the *lel*$_3$-conformations, Λ($\delta\delta\delta$) or Δ($\lambda\lambda\lambda$), whereas if each C−C bond is obliquely inclined with respect to the C_3 axis, one has the *ob*$_3$-conformation Δ($\delta\delta\delta$) or Λ($\lambda\lambda\lambda$) (see Scheme 6). We note that the *lel*$_3$-conformation Λ($\delta\delta\delta$) and the *ob*$_3$-conformation Λ($\lambda\lambda\lambda$) as diastereoisomers will have different CD spectra, and the same will be the case for Δ($\lambda\lambda\lambda$) and Δ($\delta\delta\delta$).

The 1,2-propyl-diamine ligand (pn) exists as the two enantiomers *S*-(+)-1,2-propyl-diamine and *R*-(−)-1,2-propyl-diamine, Scheme 7. As chelating ligands both enantiomers adopt a conformation with the methyl in the equatorial position, whereas the axial conformation is absent for steric reasons, Scheme 8. Due to the equatorial preference, the *S*-(+)-1,2-propyl-diamine only adopts the δ-conformation, giving rise to the *lel*$_3$-complex Λ($\delta\delta\delta$)-(+)-$[Co(S\text{-}pn)_3]^{3+}$ and the *ob*$_3$-diastereoisomer Δ($\delta\delta\delta$)-(−)-$[Co(S\text{-}pn)_3]^{3+}$. On the other hand, *R*(−)-1,2-propyl-diamine takes on the λ-conformation and forms the *lel*$_3$-complex Δ($\lambda\lambda\lambda$)-(−)-$[Co(R\text{-}pn)_3]^{3+}$ and the *ob*$_3$-diastereoisomer Λ($\lambda\lambda\lambda$)-(+)-$[Co(R\text{-}pn)_3]^{3+}$.

In the present work, TD-DFT is employed to simulate the absorption and CD spectra of Λ-$[Co(S\text{-}pn)_n(en)_{3-n}]^{3+}$, Δ-$[Co(S\text{-}pn)_n(en)_{3-n}]^{3+}$ (n = 1, 2, 3), Λ-$[Co(en)_3]^{3+}$, Δ-$[Co(en)_3]^{3+}$, Λ-$[Rh(R\text{-}pn)_3]^{3+}$, and Δ-$[Rh(R\text{-}pn)_3]^{3+}$. These data are compared with the corresponding experimental spectra.[30,31] We have

(24) Furche, F.; Ahlrichs, R.; Wachsmann, C.; Weber, E.; Sobanski, A.; Vögtle, F.; Grimme, S. *J. Am. Chem. Soc.* **2000**, *122*, 1717−1724.
(25) Autschbach, J.; Ziegler, T.; van Gisbergen, S. J. A.; Baerends, E. J. *J. Chem. Phys.* **2002**, *116*, 6930−6940.
(26) Autschbach, J.; Jorge, F. E.; Ziegler, T. *Inorg.Chem.* **2003**, *42*, 2867−2877.
(27) He, Y.; Cao, X.; Na_e, L. A.; Freedman, T. A. *J. Am. Chem. Soc.* **2001**, *123*, 11320−11321.
(28) Freedman, T. B.; Cao, X.; Young, D. A.; Na_e, L. A. *J. Phys. Chem. A* **2002**, *106*, 3560−3565.
(29) (a) Jorge, F. E.; Autschbach, J.; Ziegler, T. *Inorg. Chem.* **2003**, 42, 8902−8910. (b) Stiefel, E. I.; Brown, G. F. *Inorg. Chem.* **1972**, *11*, 434−436. (c) Corey, E. J.; Bailar, J. C. *J. Am. Chem. Soc.* **1959**, *81*, 2620−2629.
(30) Mason, S. F. Optical activity and molecular dissymmetry in coordination compounds. In *Fundamental aspects and recent developments in optical rotatory dispersion and circular dichroism*; Ciardelli, F., Salvatory, P., Eds; Heyden and Son Ltd.: London, 1973.
(31) Hearson, J. A.; Mason, S. F.; Wood, J. W. *Inorg. Chim. Acta* **1977**, *23*, 95−96.

Scheme 3. Polar Distortion of the Octahedron

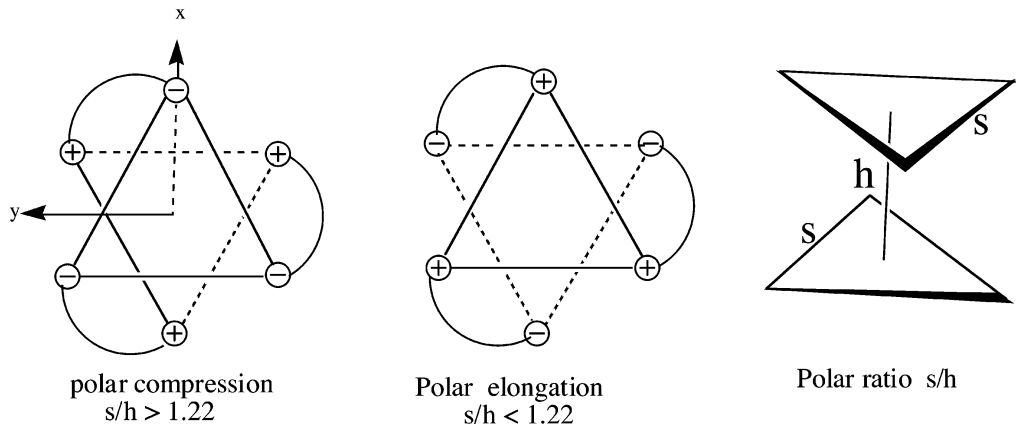

Scheme 4. Azimuthal Distortion of Octahedron

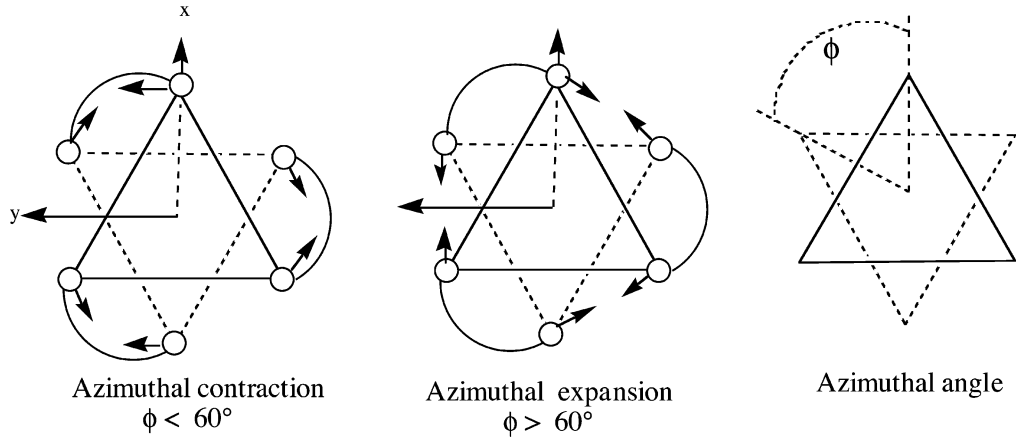

Scheme 5. λ and δ Enantiomeric Ligand Conformations[a]

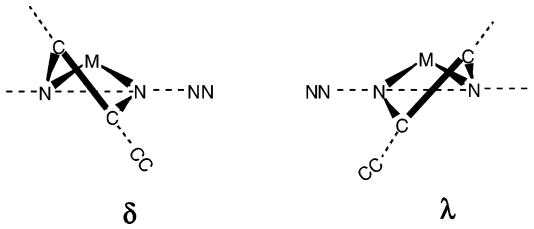

[a] Dotted line indicates NN direction.

Scheme 6. *lel* and *ob* Ligand Orientations

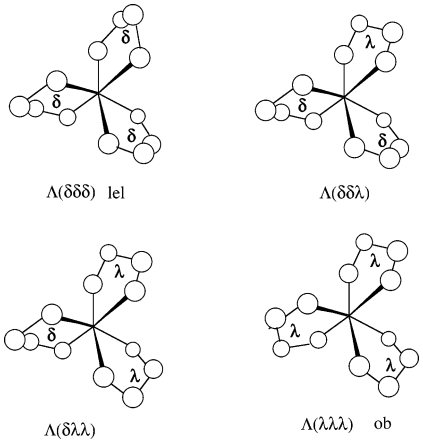

chosen these systems because of the available experimental data and because Λ-$[Co(S\text{-}en)_n(en)_{3-n}]^{3+}$ and Δ-$[Co(S\text{-}pn)_n(en)_{3-n}]^{3+}$ ($n = 1, 2, 3$) as well as Λ-$[Rh(R\text{-}pn)_3]^{3+}$ and Δ-$[Rh(R\text{-}pn)_3]^{3+}$ have the potential to form pairs of diastereoisomers according to the discussion above. By comparing their CD spectra it is thus possible to study the configurational and conformational effects observed in CD spectra of Co(III) tris-diamine complexes for both d−d and CT transitions through the different influence exerted by diamine chains in their *ob*- and *lel*-conformations.

The computational details are summarized in section 2. In section 3 the CD spectra are presented and compared with experimental data when available from the literature. Finally the conclusions of this work are given in section 4.

Computational Details

The calculations have been carried out with a modified version of the Amsterdan density functional (ADF) program.[32−34] It contains the methodology for the computation of optical rotations and CD spectra[25,35,36] implemented in the previously developed TD-DFT code.[37−39] It is currently restricted to closed shell ground states. From the calculated singlet excitation energies and associated oscillator-, and rotatory strengths, spectra have been simulated and compared with experimental data. The empirical recipe of Brown et al.[40] for the line

(32) Fonseca Guerra, C.; Visser, O.; Snijders, J. G.; te Velde, G.; Baerends, E. J. Parallelisation of the Amsterdam Density Functional program Program. In *Methods and Techniques for Computational Chemistry*; STEF: Cagliari, 1995.
(33) te Velde, G.; Bickelhaupt, F. M.; Baerends, E. J.; van Gisbergen, S. J. A.; Fonseca Guerra, C.; Snijders, J. G.; Ziegler, T. *J. Comput. Chem.* **2001**, *22*, 931−967.
(34) Amsterdam Density Functional program, Theoretical Chemistry, Vrije Universiteit, Amsterdam, URL: http://www.scm.com.
(35) Autschbach, J.; Ziegler, T. *J. Chem. Phys.* **2002**, *116*, 891−896.
(36) Autschbach, J.; Ziegler, T.; Patchkovskii, S.; van Gisbergen, S. J. A.; Baerends, E. J. *J. Chem. Phys.* **2002**, *117*, 581−592.

Scheme 7. Different Diene Ligands

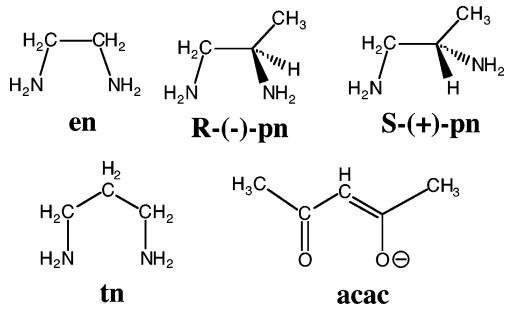

Scheme 8. Axial and Equatorial Orientations of the Methyl Group in Coordinated *S*-(+)-1,2-Propyl-diamine and *R*-(−)-1,2-Propyl-diamine[a]

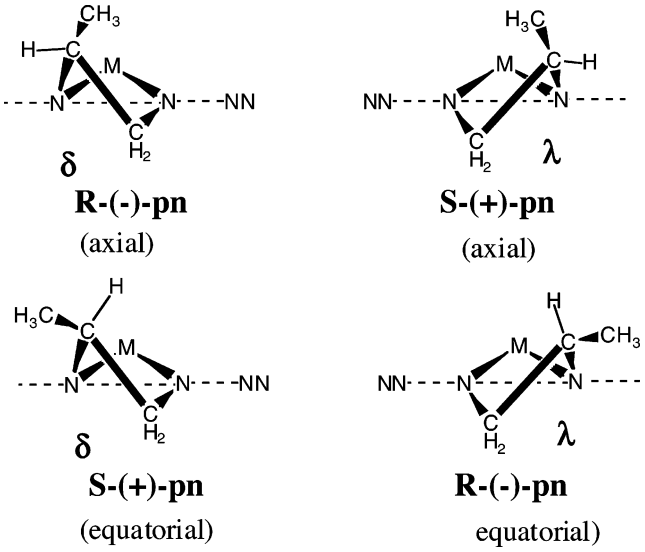

[a] Dotted line indicates NN direction.

widths has been employed which yields a reasonable overall agreement with experiments [$\Delta\bar{\nu} = 7.5.\sqrt{\bar{\nu}}$, with $\bar{\nu}$ in cm^{-1}]. Numerical data for the experimental spectra have been extracted from graphical material available in the literature with the "g3data" software.[41] The small, frozen, core-valence triple-ζ polarized "TZP" Slater basis sets of the ADF database have been employed in all calculations. The dipole-length formula has been used to compute the rotatory strengths, since it has been shown[26] for $[Co(en)_3]^{3+}$ that the results obtained with this approach are in good agreement with those calculated with the dipole-velocity formula.

We have found[26] that reasonable agreement with experimental spectra for the +3 charged complexes only can be achieved if solvation is taken into account in the calculation. On the other hand, solvation is only of minor importance for neutral or singly charged complexes. Thus, the "COnductor-like continuum Solvent MOdel" (COSMO)[42,43] has been applied in all calculations presented here. Features due to fine structure splitting of the energy levels, such as molecular vibrations, are neglected in the present study.

The results presented in the next sections are based on the Vosko−Wilk−Nusair[44] (VWN) local density approximation (LDA) with the Becke88−Perdew86 (BP86) gradient corrections.[45,46] The use of other pure density functionals does not significantly change the simulated spectra.[26] We find for the charged Co complexes that the energies of the weak d-to-d transitions are systematically overestimated, whereas the CT excitation energies are underestimated. These errors are much smaller for the homologous 4d complex $[Rh(pn)_3]^{3+}$, in line with previous studies.[26,29a] The origin of the errors for 3d complexes have been discussed extensively elsewhere.[26] The use of an asymptotically corrected Kohn−Sham potential did not lead to an improvement of the results in comparison with experiment, since the experimentally accessible range of the CD spectra is determined by valence excitations. All TD-DFT calculations have been carried out based on optimized geometries (VWN functional and TZP basis sets). For a quantitative comparison between experimental and simulated CD spectra, all tris-diamine complexes shown in Figures 1 and 2, have had their calculated excitation energies shifted by -5.4×10^3 cm^{-1} in the d-to-d transition region ($<35 \times 10^3$ cm^{-1}) and by 6.2×10^3 cm^{-1} in the CT region ($<35 \times 10^3$ cm^{-1}). We should point out that these shifts are only applied to facilitate the graphical comparison of the simulated and experimental spectra. Generally,[26] we have found that all main characteristics of the CD spectra are correctly reproduced by the computations.

In TD-DFT we can in general express[25] rotatory strengths corresponding to the transition $0 \rightarrow \lambda$ as

$$R(0\rightarrow\lambda) = \sum_{i}^{occ}\sum_{a}^{vir} A_{ia}^{\lambda}\langle\psi_i|\vec{P}|\psi_a\rangle \cdot \sum_{j}^{occ}\sum_{b}^{vir} B_{jb}^{\lambda}\langle\psi_j|\vec{M}|\psi_b\rangle \qquad (1)$$

where A_{ia}^{λ} and B_{bj}^{λ} are vectors associated with the transition $0 \rightarrow \lambda$ and spanned by the basis set of occupied $\{\psi_{k;\ k=,occ}\}$, $k = i, j$ and virtual $\{\psi_{c;c=occ+1,vir}\}$ $c = a, b$ orbitals. The vectors **A** and **B** are further determined by solving a set of coupled differential equations.[25] The sum over *i*,*a* containing the electric dipole operator $\vec{P} = \vec{r}$ is related to the electric transition dipole moment (ETDM), whereas the sum over *j*,*b* containing the magnetic dipole moment $\vec{M} = -i/2\hbar(\vec{r} \times \vec{\nabla})$ is related to the magnetic transition dipole moment (MTDM). In the ADF program it is further possible to use symmetrized linear combinations of ligand orbitals (occupied and virtual) as well as metal orbitals (occupied and virtual) as a basis set $\{\chi_\mu,\chi_\nu\}$. On this basis the rotatory strength reads

$$R(0\rightarrow\lambda) = \sum_{\mu,\nu} C_\mu \upsilon^{\lambda}\langle\chi_\mu|\vec{P}|\chi_\nu\rangle \sum_{\mu,\nu} D_\mu \upsilon^{\lambda}\langle\chi_\mu|\vec{M}|\chi_\nu\rangle \qquad (2)$$

where the vectors **C** and **D** are readily derived from the **A**,**B** vectors and the molecular orbital coefficients in the basis $\{\chi_\mu,\chi_\nu\}$. It is thus possible from inspection of eq 2 to determine what combinations of $\{\chi_\mu,\chi_\nu\}$ will contribute to $R(0\rightarrow\lambda)$.

The energy gaps between occupied and virtual orbitals serve as a zero-order estimate for the excitation energies.[10] The Davidson algorithm is employed to obtain a number of singlet and triplet excitation energies. The transitions are calculated independently for each irreducible representation of the molecule's point group. The $[Co(en)_3]^{3+}$ complex has D_3 symmetry, whereas the $[Co(pn)_3]^{3+}$ and $[Rh(pn)_3]^{3+}$ complexes have C_3 symmetry. As the ADF program[32−34] cannot handle C_3 symmetry, complexes of this symmetry plus $[Co(pn)(en)_2]^{3+}$ and $[Co(pn)_2(en)]^{3+}$ are treated without symmetry. However, for $[Co(pn)_3]^{3+}$ and $[Rh(pn)_3]^{3+}$ the resulting orbitals still contain C_3 symmetry; as a result, the simulated spectra can be assigned according to that point group.

Results and Discussion

Conformational Preferences for the Diene Ligands in Co(III) and Rh(III) Tris(bidentate) Complexes. For $[Co(en)_3]^{3+}$,

(37) van Gisbergen, S. J. A.; Snijders, J. G.; Baerends, E. J. *J. Chem. Phys.* **1995**, *103*, 9347−9354.
(38) van Gisbergen, S. J. A.; Snijders, J. G.; Baerends, E. J. *Comput. Phys. Commun.* **1999**, *118*, 119−138.
(39) van Gisbergen, S. J. A.; Fonseca-Guerra, C.; Baerends, E. J. *J. Comput. Chem.* **2000**, *21*, 1511−1523.
(40) Brown, A.; Kemp, C. M.; Mason, S. F. *J. Chem. Soc. (A)* **1971**, 751−755.
(41) Frantz, J. "g3data", 2002 URL: http://beam.helsinki._/_frantz/software/g3data.php.
(42) Klamt, A.; Schüürmann, G. *J. Chem. Soc., Perkin Trans. 2* **1993**, 799−805.
(43) Pye, C. C.; Ziegler, T. *Theor. Chem. Acc.* **1999**, *101*, 396−408.
(44) Vosko, S. H.; Wilk, L.; Nusair, M. *Can. J. Phys.* **1980**, *58*, 1200−1211.
(45) Becke, A. D. *Phys. Rev. A* **1988**, *38*, 3098−3100.
(46) Perdew, J. P. *Phys. Rev. B* **1986**, *33*, 8822−8824.

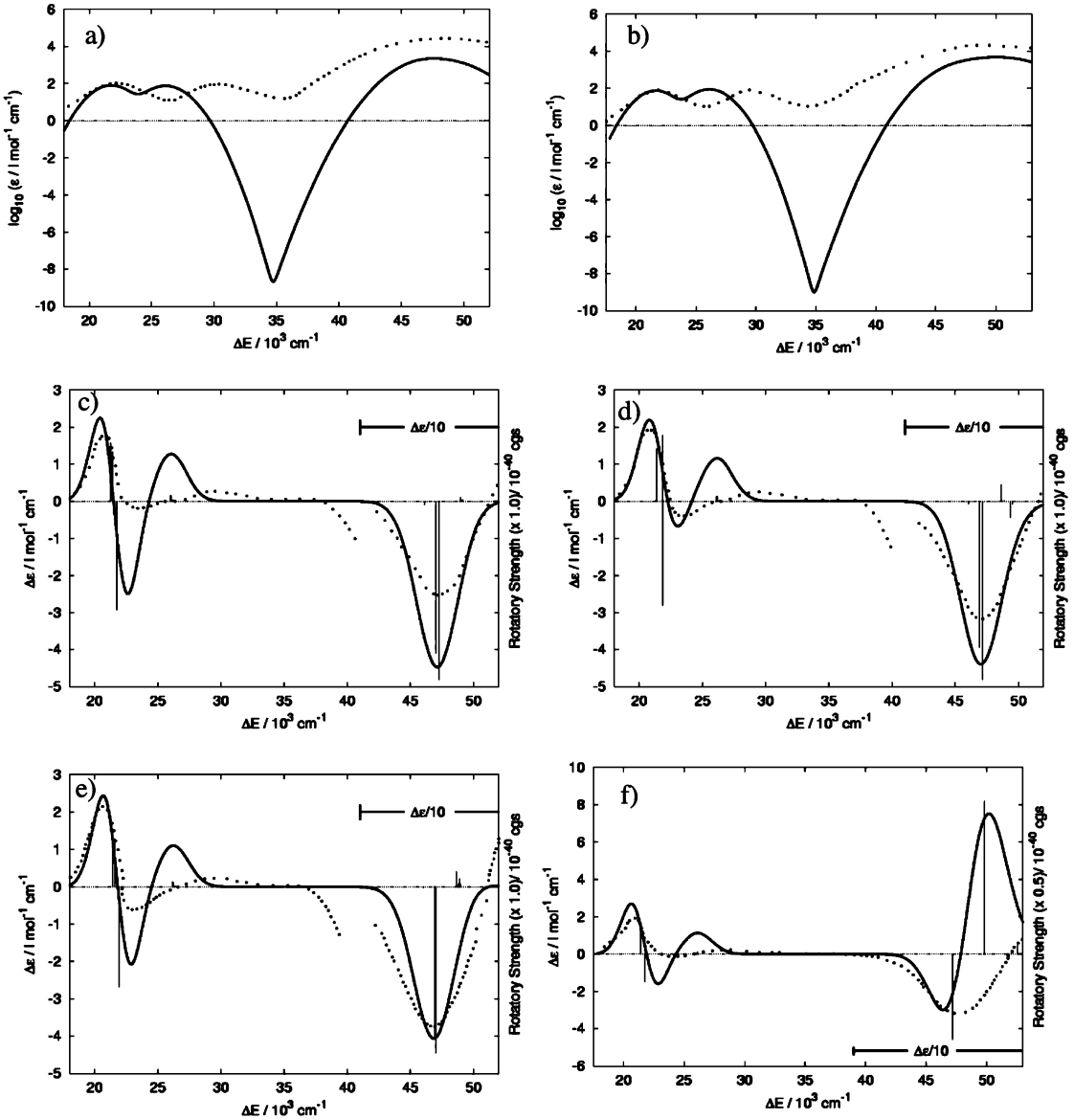

Figure 1. Experimental and simulated (solid lines) absorption spectra of (a) $\Lambda(\delta\delta\delta)$-(+)-$[Co(S\text{-}pn)_n(en)_{3-n}]^{3+}$ (n = 1, 2, 3) and (b) $\Lambda(\delta\delta\delta)$-(+)-$[Co(en)_3]^{3+}$. CD spectra of (c) $\Lambda(\delta\delta\delta)$-(+)-$[Co(S\text{-}pn)(en)_2]^{3+}$, (d) $\Lambda(\delta\delta\delta)$-(+)-$[Co(S\text{-}pn)_2en]^{3+}$, (e) $\Lambda(\delta\delta\delta)$-(+)-$[Co(S\text{-}pn)_3]^{3+}$, and (f) $\Lambda(\delta\delta\delta)$-(+)-$[Co(en)_3]^{3+}$ in water. Excitation energies and rotatory strengths are plotted as vertical bars. For all complexes, theoretical excitation energies smaller and larger than 35 $\times$ 10^3 cm^{-1} are shifted by -5.4×10^3 cm^{-1} and by 6.2×10^3 cm^{-1}, respectively. Experiment is dotted lines and theory is solid lines.

Corey and Bailar[29b] employed a simple force field[29b] analysis to estimate that the *lel*$_3$-form was more stable than the *ob*$_3$-conformation by 1.8 kcal/mol, Scheme 6. Thermodynamic studies have further[48] demonstrated that the distribution between the possible ring conformations in Λ-$[Co(en)_3]^{3+}$ is 59% [$\delta\delta\delta$ (*lel*$_3$)], 29% [$\delta\delta\lambda$ (*lel*$_2$*ob*)], 8% [$\delta\lambda\lambda$ (*lelob*$_2$)], and 4% [$\lambda\lambda\lambda$ (*ob*$_3$)], respectively, in aqueous solution at 25 °C. Our DFT calculations predict for $[Co(en)_3]^{3+}$ in water that *lel*$_3$ is more stable than *ob*$_3$ by 1.5 kcal/mol, in good agreement with the estimate due to Corey and Bailar.[47] X-ray diffraction studies always find $[Co(en)_3]^{3+}$ to adopt the *lel*$_3$-conformation.

The 1,2-propyl-diamine ligand (pn) exists as the two enantiomers *S*-(+)-1,2-propyl-diamine and *R*-(−)-1,2-propyl-diamine, Scheme 7. As chelating ligands both enantiomers adopt a conformation with the methyl in the equatorial position, whereas the axial conformation is absent for steric reasons, Scheme 8. Thus, Corey and Bailar[29b] found from a simple force field[47b] analysis that the equatorial position is preferred by 2 kcal/mol for each methyl group. Our calculations confirm the equatorial preference in $[Co(S\text{-}pn)_3]^{3+}$ where the change to the axial position of all three methyl groups requires 16.5 kcal/mol in solution. Due to the equatorial preference, the *S*-(+)-1,2-propyl-diamine only adopts the δ-conformation giving rise to the *lel*$_3$-complex $\Lambda(\delta\delta\delta)$-(+)-$[Co(S\text{-}pn)_3]^{3+}$ and the *ob*$_3$-diastereoisomer $\Delta(\delta\delta\delta)$-(−)-$[Co(S\text{-}pn)_3]^{3+}$. On the other hand, *R*(−)-1,2-propyl-diamine takes on the λ-conformation and forms the *lel*$_3$-complex $\Delta(\lambda\lambda\lambda)$-(−)-$[Co(R\text{-}pn)_3]^{3+}$ and the *ob*$_3$-diastereoisomer $\Lambda(\lambda\lambda\lambda)$-(+)-$[Co(R\text{-}pn)_3]^{3+}$.

Dwyer et al.[48−50] have carried out equilibrium studies of $[Co(S\text{-}pn)_3]^{3+}$ in aqueous solution at 25° C where they find that

(47) Mason E. A.; Kreevoy *J. Am. Chem. Soc.* **1955**, *77*, 5808−5814.
(48) Dwyer, F. P.; Garvan, F. L.; Shulman, L. *J. Am. Chem. Soc.* **1959**, *81*, 290−294.
(49) Dwyer, F. P.; MacDermott, T. E.; Sargeson, A. M. *J. Am. Chem. Soc.* **1963**, *85*, 2913−2916.
(50) Dwyer, F. P.; Sargeson, A. M.; James, L. B. *J. Am. Chem. Soc.* **1964**, *86*, 590−592.

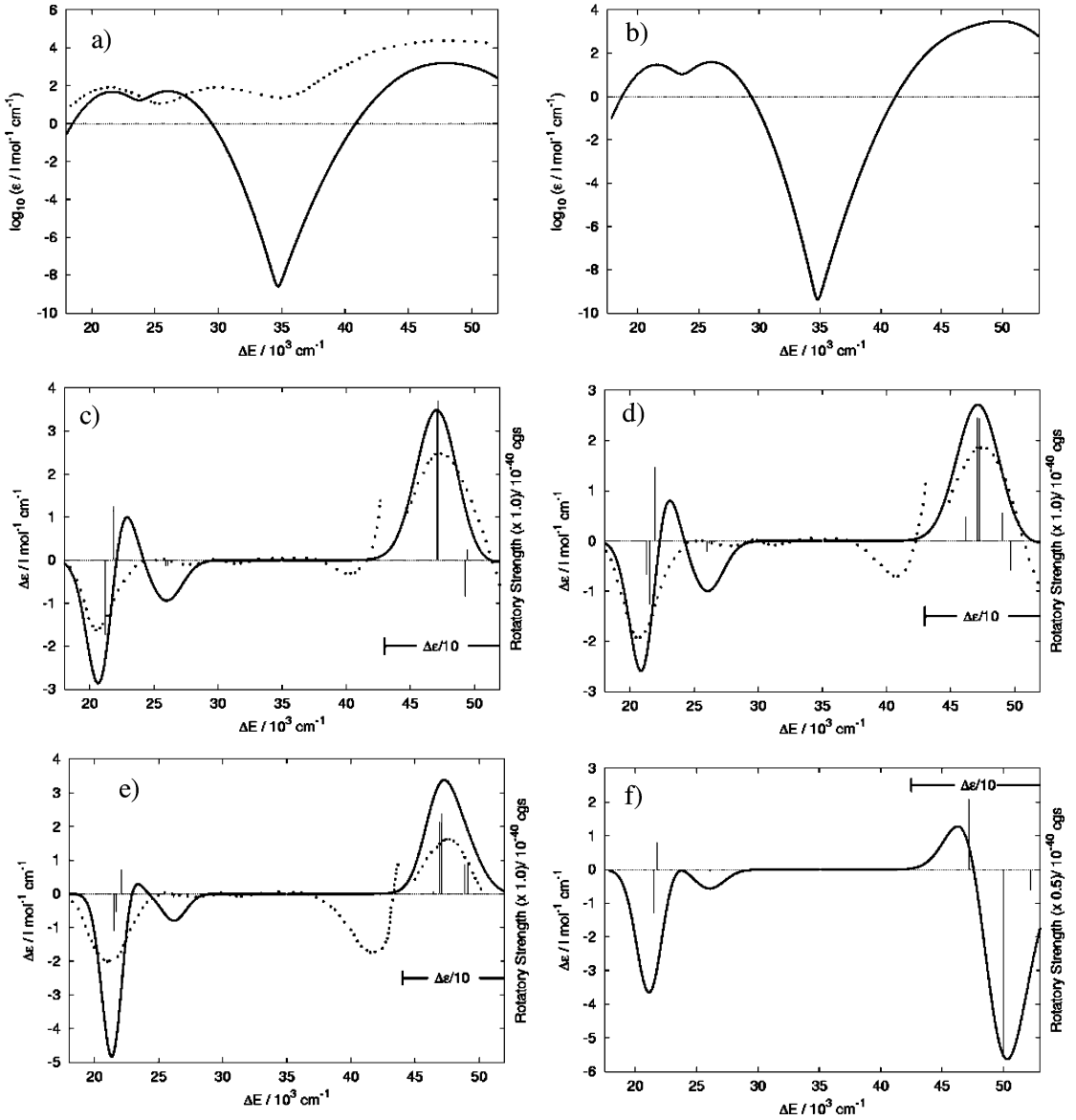

Figure 2. Experimental and simulated absorption spectra of (a) Δ-((δ)$_n$(λ)$_{3-n}$)-(−)-[Co(S-pn)$_n$(en)$_{3-n}$]$^{3+}$ (n = 1, 2, 3) and (b) Δ-($\delta\delta\delta$)-(−)-[Co(en)$_3$]$^{3+}$. CD spectra of (c) Δ-(δ(λ)$_2$)-(−)-[Co(S-pn)(en)$_2$]$^{3+}$, (d) Δ-((δ)$_2\lambda$)-(−)-[Co(S-pn)$_2$en]$^{3+}$, (e) Δ-($\delta\delta\delta$)-(−)-[Co(S-pn)$_3$]$^{3+}$, and (f) Δ-($\delta\delta\delta$)-(−)-[Co(en)$_3$]$^{3+}$ in water. Excitation energies and rotatory strengths are plotted as vertical bars. For all complexes, theoretical excitation energies smaller and larger than 35 × 10^3 cm^{-1} are shifted by −5.4 × 10^3 cm^{-1} and by 6.2 × 10^3 cm^{-1}, respectively. Experiment is dotted lines and theory is solid lines.

the *lel*$_3$-complex $\Lambda(\delta\delta\delta)$-(+)-[Co(S-pn)$_3$]$^{3+}$ is more stable than the *ob*$_3$-diastereoisomer $\Delta(\delta\delta\delta)$-(−)-[Co(S-pn)$_3$]$^{3+}$ by 1.6 kcal/mol. We calculate a similar preference for *lel*$_3$ of 1.7 kcal/mol. The X-ray diffraction studies of Saito et al.[51] show that crystals of [Co(S-pn)$_3$]$^{3+}$ contain both the *lel*$_3$-complex, $\Lambda(\delta\delta\delta)$-(+)-[Co(pn)$_3$]$^{3+}$, as well as the *ob*$_3$-diastereoisomer, $\Delta(\delta\delta\delta)$-(−)-[Co(S-pn)$_3$]$^{3+}$.

It follows from the discussion above that the mixed complexes [Co(en)(S-pn)$_2$]$^{3+}$ and [Co(en)$_2$S-pn]$^{3+}$ in the Λ configuration will be present primarily in the *lel*$_3$ forms $\Lambda(\delta\delta\delta)$-(+)-[Co(en)(S-pn)$_2$]$^{3+}$ and $\Lambda(\delta\delta\delta)$-(+)-[Co(en)$_2$S-pn]$^{3+}$. For the Δ configuration of the same complexes ethylenediamine will prefer the *lel* λ-conformation whereas S-pn takes on the *ob* δ-conformation with the methyl group in the equatorial position, Scheme 8. The preferred structures will as a consequence be the *lelob*$_2$-conformation $\Delta(\lambda\delta\delta)$-(−)-[Co(en)(S-pn)$_2$]$^{3+}$ and the *lel*$_2$*ob*-conformation $\Delta(\lambda\lambda\delta)$-(−)-[Co(en)$_2$S-pn]$^{3+}$. Dwyer et al.[48−50] found from equilibrium studies that $\Lambda(\delta\delta\delta)$-(+)-[Co(en)(S-pn)$_2$]$^{3+}$ was 0.45 kcal/mol more stable than the diastereoisomer $\Delta(\lambda\delta\delta)$-(−)-[Co(en)(S-pn)$_2$]$^{3+}$, whereas $\Lambda(\delta\delta\delta)$-(+)-[Co(en)$_2$S-pn]$^{3+}$ is 1.2 kcal/mol more stable than the diastereoisomer $\Delta(\lambda\lambda\delta)$-(−)-[Co(en)$_2$S-pn].$^{3+}$ The corresponding numbers calculated in this study are 0.6 and 1.8 kcal/mol, respectively.

Calculated and Experimental CD Spectra. We display in Figures 1 and 2 the computed excitation energies and rotatory strengths along with experimental[30,31] and simulated absorption and CD spectra for all Co(III) complexes discussed here. The position of the excitations and their rotatory strength are indicated by bars. Unless stated otherwise, both theoretical and experimental spectra refer to the condensed phase with water as the solvent. Thus, in understanding the experimental spectra it is important to note that each en-ring in solution might adopt the more favorable *lel* λ-conformation for complexes of the Δ-

(51) Saito, Y. *Pure Appl. Chem.* **1968**, *17*, 21−36.

Table 1. Calculated d−d Rotatory Strengths and Structural Parameters for $[Co(en)_n(S\text{-}pn)_{n-3}]^{3+}$ ($n = 0,1,2,3$)

	real system		model system[c]			
complex	$R(E)$[a,b]	$R(A)$	$R(E)$	$R(A)$	s/h[d]	$\Delta\phi$[e]
$\Lambda(\delta\delta\delta)$-(+)-$Co(en)_3$	29.9	−33.0	36.0	−34.8	1.28	− 6.25
$\Delta(\delta\delta\delta)$-(−)-$Co(en)_3$	−25.7	16.0	−21.4	19.8	1.31	4.57
$\Lambda(\delta\delta\delta)$-(+)-$Co(S\text{-}pn)(en)_2$	27.6	−21.5	24.8	−24.2	1.27	−6.73
$\Delta(\delta\lambda\lambda)$-(−)-$Co(S\text{-}pn)(en)_2$	−17.5	12.5	−17.6	−18.1	1.29	5.82
$\Lambda(\delta\delta\delta)$-(+)$Co(S\text{-}pn)_2en$	32.1	−28.1	26.9	−26.6	1.27	−6.86
$\Delta(\delta\delta\lambda)$-(−)$Co(R\text{-}pn)_2en$	−19.5	14.7	−12.5	12.6	1.31	4.02
$\Lambda(\delta\delta\delta)$-(+)-$Co(S\text{-}pn)_3$	28.3	−27.0	22.3	−22.2	1.27	−7.20
$\Delta(\delta\delta\delta)$-(−)-$Co(R\text{-}pn)_3$	−16.6	7.2	−9.9	10.4	1.33	4.32

[a] Rotatory strengths in 10^{-40} cgs units. [b] Sum over two E components. [c] The model system was $Co(NH_3)_6$. For each "real" system $[Co(en)_n(S\text{-}pn)_{n-3}]^{3+}$ ($n = 0, 1, 2, 3$), the geometry of the corresponding model system $Co(NH_3)_6$ was constructed by changing each carbon chain by two hydrogen atoms. [d] Polar ratio, see Scheme 3. [e] Deviation of azimuthal angle from the "octahedral" value of 60°, see Scheme 9.

configuration and the more favorable *lel* δ-conformation for the Λ-configuration. On the other hand, the S-pn- and R-pn-rings always adopt respectively the δ- and λ-conformation with the methyl group of propylenediamine in the equatorial position, Scheme 8.

Figure 1 presents the spectra for $\Lambda(\delta\delta\delta)$-(+)-$[Co(S\text{-}pn)_n(en)_{3-n}]^{3+}$ ($n = 1, 2, 3$) whereas the corresponding data for Δ-$((\delta)_n(\lambda)_{3-n})$-(−)-$[Co(S\text{-}pn)_n(en)_{3-n}]^{3+}$ ($n = 1, 2, 3$) are given in Figure 2. Thus, a comparison of the two figures for $n = 1$, 2, 3, respectively, makes it possible to study how the CD spectra (aside from a trivial change in sign) is modified by transforming the S-pn-ring from the *lel* δ-conformation in $\Lambda(\delta\delta\delta)$-(+)-$[Co(S\text{-}pn)_n(en)_{3-n}]^{3+}$ ($n = 1, 2, 3$) (Figure 1) to the *ob* δ-conformation in Δ-$((\delta)_n(\lambda)_{3-n})$-(−)-$[Co(S\text{-}pn)_n(en)_{3-n}]^{3+}$ (Figure 2). A similar examination can be conducted for the en-ring by comparing the CD-spectrum of $\Lambda(\delta\delta\delta)$-(+)-$[Co(en)_3]^{3+}$ in Figure 1 with the (purely theoretical) CD-spectrum of Δ-$(\delta\delta\delta)$-(−)-$[Co(en)_3]^{3+}$ in Figure 2.

CD Spectra in the d-to-d Transition Region for Λ-$[Co(S\text{-}pn)^n(en)_{3-n}]^{3+}$ and Δ-$[Co(S\text{-}pn)_n(en)_{3-n}]^{3+}$ with $n = 0, 1, 2, 3$. Figure 1 displays the simulated and observed absorption and CD spectra for $\Lambda(\delta\delta\delta)$-(+)-$[Co(S\text{-}pn)_n(en)_{3-n}]^{3+}$ ($n = 0$, 1, 2, 3). We notice in all cases in the d-to-d transition region of the CD spectrum a positive band at lower energy ($\sim 20 \times 10^3$ cm^{-1}). It follows from our calculations that this band is of E-symmetry and originates from the d-to-d transition $^1A_1 \rightarrow {}^1E$ where ^1E is of $^1T_{1g}$ O_h parentage , see Table 1 and Scheme 1. Such an assignment has also been reached experimentally for $n = 0$ and 3. The simulated spectra reveals in addition in the same region at slightly higher energies a positive band of A_2 or A symmetry originating from the $^1A_1 \rightarrow {}^1A_2$ or $^1A_1 \rightarrow {}^1A$ d-to-d transitions where $^1A_2$ (or ^1A) is of $^1T_{1g}$ O_h parentage, see Table 1 and Scheme 1. The A-band is only barely noticeable in the experimental spectra except for $n = 3$, presumably because it is overlaid by the E-band. That this is so has been confirmed experimentally by single crystal CD-spectroscopy ($n = 0$, 3) where the two bands can be obtained separately and the A-band clearly is present at marginally higher energies ($\sim$ 500 cm^{-1}) than the E-band.[52,53] A positive weak band at $\sim 26 \times 10^3$ cm^{-1} is revealed by experiment as well as theory. It has a low intensity since it corresponds to the d-to-d transition $^1A_1 \rightarrow {}^1E$ where ^1E is of $^1T_{2g}$ O_h parentage with the corresponding $^1A_{1g} \rightarrow {}^1T_{2g}$ transition being both magnetically and electrically forbidden , see Scheme 1.

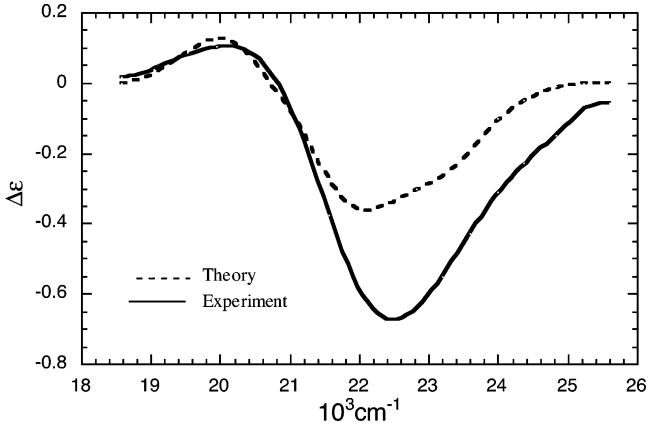

Figure 3. One-sixth of the addition of the CD spectra of $\Lambda(\delta\delta\delta)$-(+)-$[Co(S\text{-}pn)_3]^{3+}$ and Δ-$(\delta\delta\delta)$-(−)-$[Co(S\text{-}pn)_3]^{3+}$. Experiment is solid lines and theory is dotted lines.

Figure 2 displays the simulated and observed absorption and CD spectra for $\Delta((\delta)_n(\lambda)_{3-n})$-(−)-$[Co(S\text{-}pn)_n(en)_{3-n}]^{3+}$ ($n = 1$, 2, 3) and $\Delta(\delta\delta\delta)$-(−)-$[Co(en)_3]^{3+}$. It is clear that the CD spectra in Figures 1 and 2 for the same n not only differ in sign but also, in absolute terms, have different rotatory strengths for the same transitions. This is underlined in Figure 3 where we present the sum of the spectra for the stereoisomers $\Lambda(\delta\delta\delta)$-(+)-$[Co(S\text{-}pn)_3]^{3+}$ and $\Delta(\delta\delta\delta)$-(−)-$[Co(S\text{-}pn)_3]^{3+}$. The experimental and simulated addition spectra are qualitatively similar not only for $n = 3$ as shown in Figure 3 but also for $n = 1$, 2. The shape of the difference spectrum is consistent with that the rotatory strengths for the isomer $\Lambda(\delta\delta\delta)$-(+)-$[Co(S\text{-}pn)_3]^{3+}$ in absolute terms are larger than for the isomers $\Delta(\delta\delta\delta)$-(−)-$[Co(S\text{-}pn)_3]^{3+}$, as seen for the computational results reported in Table 1. Similar relations are seen to hold for $n = 1$, 2, as well as between Λ-$(\delta\delta\delta)$-(+)-$[Co(en)_3]^{3+}$ and $\Delta(\delta\delta\delta)$-(−)-$[Co(en)_3]^{3+}$, Table 1.

To understand this trend, we shall consider a simplified model[29a] of our complexes in which we represent the three diamine rings by six occupied nitrogen based σ-orbitals. We shall in addition allow the six nitrogen centers, Scheme 9, to be displaced from octahedral O_h symmetry to D_{3d} symmetry by a polar compression or elongation, Scheme 3, to the nuclear geometry q^o.

In this simplified model, the d−d transitions under consideration are caused by excitation from the metal-based HOMOs ($1e_{ga}$,$1e_{gb}$, and $1a_{1g}$) of t_{2g} parentage in O_h symmetry to the metal-based LUMOs ($2e_{ga}$,$2e_{gb}$) of e_g parentage in O_h symmetry, Scheme 1. We can thus write[29a] for the rotatory strengths

$$R(A_{2g}) \propto \langle 1e_{ga}|\vec{P}|2e_{gb}\rangle\langle 2e_{gb}|\vec{M}|1e_{ga}\rangle \qquad (3a)$$

$$R(E) \propto \langle 1e_{ga}|\vec{P}|2e_{ga}\rangle\langle 2e_{ga}|\vec{M}|1e_{ga}\rangle \qquad (3b)$$

In this expression the HOMOs can be written as a pure metal-based d-orbital $M_\pi(e_{gc})$, see Table 2. Thus,

$$1e_c = M_\pi(e_{gc}) \quad (c = a, b) \qquad (4a)$$

On the other hand,the LUMOs are made up of d-orbitals M_σ-

(52) Mason S. F.; Peart, B. J. *J. Chem. Soc. Dalton Trans.* **1977**, 937−941.
(53) Kuroda, R.; Saito, Y. *Bull. Chem. Soc. Jpn.* **1976**, *49*, 433−436

Table 2. Metal d-Orbitals and Ligand σ-Orbitals Symmetrized According to the D_{3d} Point Group

symmetry combinations of σ-type ligand orbitals[a,b]	metal symmetry orbitals[c]
$L_\sigma(a_{1g}) = 1/\sqrt{6}\,\{\sigma_1 + \sigma_2 + \sigma_3 + \sigma_4 + \sigma_5 + \sigma_6\}$	$M_\pi(a_{1g}) = d_{z^2}$
$L_\sigma(a_{2u}) = 1/\sqrt{6}\,\{\sigma_1 + \sigma_2 + \sigma_3 - \sigma_4 - \sigma_5 - \sigma_6\}$	$M_\pi(e_{ga}) = \sqrt{2/3}d_{x^2-y^2} + \sqrt{1/3}d_{yz}$
$L_\sigma(e_{ga}) = 1/\sqrt{12}\,\{\sigma_1 + \sigma_2 - 2\sigma_3 + \sigma_4 - 2\sigma_5 + \sigma_6\}$	$M_\pi(e_{gb}) = \sqrt{1/3}d_{xz} + \sqrt{2/3}d_{xy}$
$L_\sigma(e_{gb}) = 1/2\{-\sigma_1 + \sigma_2 - \sigma_4 + \sigma_6\}$	$M_\sigma(e_{ga}) = \sqrt{1/3}d_{x^2-y^2} - \sqrt{2/3}d_{yz}$
$L_\sigma(e_{ua}) = 1/2\{\sigma_1 - \sigma_2 - \sigma_4 + \sigma_6\}$	$M_\sigma(e_{gb}) = \sqrt{2/3}d_{xz} - \sqrt{1/3}d_{xy}$
$L_\sigma(e_{ub}) = 1/\sqrt{12}\,\{\sigma_1 + \sigma_2 - 2\sigma_3 - \sigma_4 + 2\sigma_5 - \sigma_6\}$	

[a] Numbering schemes for ligands are shown in Scheme 9. [b] The symbols σ_i $\{i = 1, 6\}$ represent the HOMOs of the six NH_3 ligands. Each HOMO is a σ-type lone pair pointing along the M−N bond vector. [c] The five d-orbitals.

Scheme 9. Numbering of Nitrogen Atoms in Tris-diamine Complexes

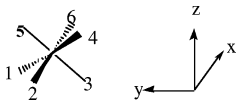

Scheme 10. Generation of an Overlap between the Odd Ligand Combination $L_\sigma(e_{ua})$ and the Even $M_\pi(e_{ga})$ Metal d-Orbital Due to an Azimuthal Distortion of the Octahedron

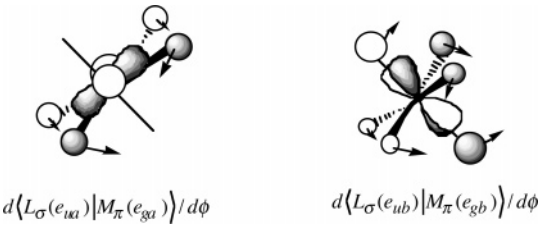

(e_{gc}) with an out-of-phase antibonding ligand contribution L_σ-(e_{gc}), see Table 2. Thus

$$2e_c = M_\sigma(e_{gc}) - C_{L_\sigma}L_\sigma(e_{gc}) \quad (c = a, b) \tag{4b}$$

where C_{L_σ} is a positive mixing coefficient. It is thus clear that the magnetic part of the expression in eq 3 will be non-zero through the contributions from the d-orbitals given by $\langle M_\sigma$-(e_{gc})$|\vec{M}|M_\pi(e_{gc})\rangle$. On the other hand, the electric parts of eq 3 are zero since both e_{gc} and $2e_{gc}$ within D_{3d} symmetry are even functions and $\vec{P}$ is odd.

It is, however, possible to obtain non-zero values for the electric component by performing an azimuthal distortion, Scheme 4, of our system from the geometry at q^o of D_{3d} symmetry to the geometry $q^o + \Delta\phi$ of D_3 symmetry since such a distortion allows even metal orbitals to mix with odd ligand combinations. Of special importance for this discussion is the fact that the odd $L_\sigma(e_{uc})$ ($c = a, b$) ligand combinations, Table 2, will overlap with the even metal orbitals $M_\pi(e_{gc})$ ($c = a, b$), Scheme 10. We find thus at $q^o + \Delta\phi$ the two HOMOs have the form:[29a]

$$^1e_c = M_\pi(e_{gc}) + \Delta\phi C_{\text{mix}}L_\sigma(e_{uc})_{(q^o+\Delta\phi)} \quad (c = a, b) \tag{5a}$$

whereas the LUMO for the purpose of this discussion can be considered unchanged.

It should be noted that the index $q^o + \Delta\phi$ attached to the ligand orbitals in eq 5a indicates that the ligand combination coefficients defined in Table 2 still are the same but that the individual ligands have been displaced by $\Delta\phi$, see also Scheme 4. Further, the mixing coefficient C_{mix} is readily obtained from perturbation theory [29a] as

$$C_{\text{mix}} = \frac{\langle L_\sigma(e_{uc})_{q^o}|dh_{KS}/d\phi|M_\pi(e_{gc})\rangle - \langle L_\sigma(e_{uc})_{(q^o+\Delta\phi)}|M_\pi(e_{gc})\rangle\epsilon(M_\pi(e_{gc}))}{\epsilon(M_\pi(e_{gc})) - \epsilon(L_\sigma(e_{uc})_{q^o})} \tag{5b}$$

Thus, the mixing is mediated by a change in the (Kohn−Sham) one-electron operator $dh_{KS}/d\phi$ as well as the emergence of an overlap between the even metal orbital and the odd ligand combination, Table 2. Further $\epsilon(M_\pi(e_{gc}))$ is the energy of the even d-orbital $\epsilon(M_\pi(e_{gc}))$whereas $\epsilon(L_\sigma(e_{uc}))$ is the energy of the odd ligand combination $L_\sigma(e_{uc})$.

Keeping only leading terms afford finally the following relations

$$R(A_2) \propto \Delta\phi C_{\text{mix}}\langle L_\sigma(e_{ua})_{(q^o+\Delta\phi)}|\vec{P}|L_\sigma(e_{gb})_{q^o}\rangle\langle M_\sigma(e_{gb})|\vec{M}|M_\pi(e_{ga})\rangle \tag{6a}$$

For tris-diamine Co(III) complexes with a Λ-configuration

$$R(E) \propto \Delta\phi C_{\text{mix}}\langle L_\sigma(e_{ua})_{(q^o+\Delta\phi)}|\vec{P}|L_\sigma(e_{ga})_{q^o}\rangle\langle M_\sigma(e_{gb})|\vec{M}|M_\pi(e_{ga})\rangle \tag{6b}$$

such as the *lel*$_3$-isomer $\Lambda(\delta\delta\delta)$-(+)-$[Co(S\text{-}pn)_3]^{3+}$ one finds that the chelate bite angle N−Co−N is such that the deviation, $\Delta\phi^\Lambda$ of Scheme 11, is negative corresponding to an azimuthal contraction. On the other hand, tris-diamine Co(III) complexes with a Δ-configuration will for the same chelate bite angle N−Co−N have a positive deviation, $\Delta\phi^\Delta$ of Scheme 11, corresponding to an azimuthal expansion. Thus, for enantiomers such as $\Lambda(\delta\delta\delta)$-(+)-$[Co(S\text{-}pn)_3]^{3+}$ and $\Delta(\lambda\lambda\lambda)$-(−)-$[Co(R\text{-}pn)_3]^{3+}$ one finds $\Delta\phi^\Lambda + \Delta\phi^\Delta = 0$. However, such a relation is not valid for the *lel*$_3$ system $\Lambda(\delta\delta\delta)$-(+)-$[Co(S\text{-}pn)_3]^{3+}$ and its *ob*$_3$-stereoisomer $\Delta(\delta\delta\delta)$-(−)-$[Co(R\text{-}pn)_3]^{3+}$. In fact, the N−Co−N chelate bite angle in the *lel* -conformation is smaller than the bite angle in the *ob*$_3$-conformation, Schemes 6 and 11. As a result, the deviation $\Delta\phi^\Lambda$ of Scheme 11 for the *lel*$_3$-conformation will in absolute terms be larger than the $\Delta\phi^\Delta$ of the *ob*$_3$-stereoisomer, as it is shown in Table 1. Given that the rotatory strength is roughly proportional to $|\Delta\phi|$, eq 6, it is thus clear why the R(E) and R(A) values in absolute terms are larger for $\Lambda(\delta\delta\delta)$-(+)-$[Co(S\text{-}pn)_3]^{3+}$ than for $\Delta(\delta\delta\delta)$-(−)-$[Co(S\text{-}pn)_3]^{3+}$.

The simplified theory[29a] discussed here is based on the geometrical arrangements of the nitrogen atoms around the metal center. It only includes the diene ring to the degree that the ring conformation dictates the geometry of the nitrogens. To gauge the limits of such a theory, we have carried out

Scheme 11. Relation between Chelate Bite Angles in the Δ- and Λ-Configurations and the Azimuthal Distortions $\Delta\phi^{\Lambda}$ and $\Delta\phi^{\Delta}$

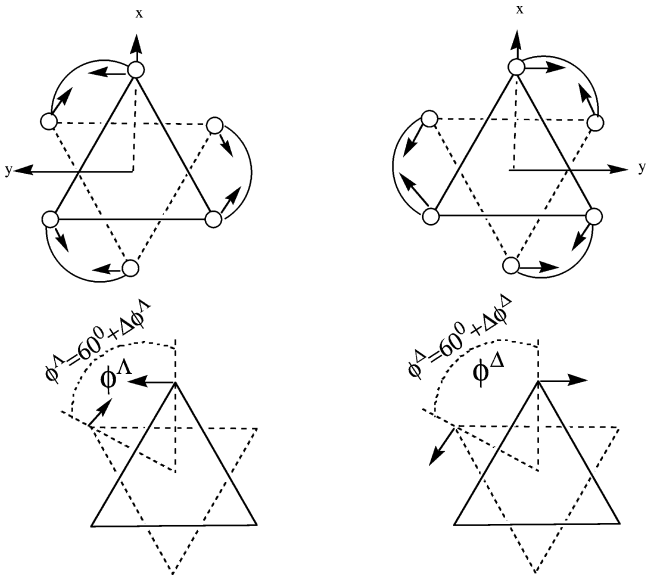

Λ-Configuration Δ-Configuration

calculations on the model system $Co(NH_3)_6^{3+}$. For each diene system in Table 1, we have constructed the corresponding model systems by replacing the C−C chains by two hydrogens, each attached to a terminal nitrogen. Thus, the diene complexes and their $Co(NH_3)_6^{3+}$ model have the same nitrogen configuration. It follows from Table 1 that the model systems exhibit the same trend as the real complexes with rotatory strengths that are larger in absolute terms for $\Lambda(\delta\delta\delta)$-(+)-$[Co(S\text{-}pn)_n(en)_{3-n}]^{3+}$ (n = 0, 1, 2, 3) than for $\Delta((\delta)_n(\lambda)_{3-n})$-(−)-$[Co(S\text{-}pn)_n(en)_{3-n}]^{3+}$ (n = 0, 1, 2, 3) with respect to a given n. This confirms that our simple analysis is qualitatively correct. That the major electrical intensity comes from elements of the type $\langle L_\sigma(e_{uc})_{(q^o+\Delta\phi)}|\vec{P}|L_\sigma(e_{gc})_{q^o}\rangle$ ($c = a, b$) was also confirmed by an analysis based on eq 2.

CD Spectra for Λ-$[Co(R\text{-}pn)_n(en)_{3-n}]^{3+}$ and Δ-$[Co(pn)^n(en)_{3-n}]^{3+}$ (n = 0, 1, 2, and 3) in the CT Region. All the $[Co(R\text{-}pn)_n(en)_{3-n}]^{3+}$ species (n = 0, 1, 2, 3) reveal in their CD spectrum an intense CD transition in the UV region (∼47 × 10^3 cm^{-1}) with a negative rotatory strength for the Λ-configuration and a corresponding positive value for the Δ-configuration, Figures 1 and 2. Our TD-DFT calculations attribute this band to the $^1A_1 \rightarrow {}^1E$ transition, see Table 3, where ^1E is of $^1T_{1u}$ O_h parentage, see Scheme 1. A crystal CD study[54] of Λ-$[Co(en)_3]^{3+}$ confirms that the first intense CT is to a state of E symmetry. The corresponding $^1A_1 \rightarrow {}^1A_2$ transition is calculated to be ∼5 × 10^3 cm^{-1} higher in energy. It only appears in Figures 1 and 2 for $[Co(en)_3]^{3+}$. However, calculated $R(A_2)$ values for all systems are given in Table 3.

It follows from the computational results presented in Table 3 that $\Lambda(\delta\delta\delta)$-(+)-$[Co(S\text{-}pn)_n(en)_{3-n}]^{3+}$ (n = 0, 1, 2, 3) for a given n has numerically larger rotatory strengths $R(A_2)$ and $R(E)$ than the stereoisomer $\Delta((\delta)_n(\lambda)_{3-n})$-(−)-$[Co(S\text{-}pn)_n(en)_{3-n}]^{3+}$ (n = 0, 1, 2, 3) for the same n. This trend can also be observed experimentally in Figures 1 and 2, especially in the case of $[Co(S\text{-}pn)_3]^{3+}$.

We can explain the trends in the CT region by the same simplified model used for the d−d transition in which we represent the three diamine rings by six occupied nitrogen-based σ-orbitals, where the nitrogen atoms initially have a geometry q^o, Scheme 9, of D_{3d} symmetry, Table 2. In this simplified model, the observed CT CD bands are caused by excitations from the ligand-based orbitals ($1e_{ua}$,$1e_{ub}$, and $1a_{2u}$) of t_{1u} parentage in O_h symmetry to the metal-based LUMOs ($2e_{ga}$,$2e_{gb}$) of e_g parentage in O_h symmetry, Scheme 1. We can thus write[29a] for the rotatory strengths

$$R(A_{2g}) \propto \langle 1e_{ua}|\vec{P}|2e_{gb}\rangle\langle 2e_{gb}|\vec{M}|1e_{ua}\rangle \quad (7a)$$

$$R(E) \propto \langle 1e_{ua}|\vec{P}|2e_{ga}\rangle\langle 2e_{ga}|\vec{M}|1e_{ua}\rangle \quad (7b)$$

In this expression the ligand-based orbitals ($1e_{ua}$,$1e_{ub}$, and $1a_{2u}$) can be written as linear combinations of nitrogen-based σ-orbitals ($L_\sigma(e_{ua})$, $L_\sigma(e_{ub})$, $L_\sigma(a_{2u})$), Table 2, whereas the metal LUMOs ($2e_{ga}$, $2e_{gb}$) can be written in the form given in eq 4b. It is thus clear that the electric part of the expression in eq 7 will be nonzero through the contributions from the ligand-based orbitals given by $C_{L_\sigma}\langle L_\sigma(e_{uc})|\vec{P}|L_\sigma(e_{gc})\rangle$. On the other hand, the magnetic parts of eq 7 are zero since $\vec{M}$ and $2e_{gc}$ within D_{3d} symmetry are even functions and e_{uc} is odd.

It is however possible to obtain non-zero values for the magnetic component by performing an azimuthal distortion, Scheme 4, of our system from the geometry at q^o of D_3 symmetry to the geometry $q^o + \Delta\phi$ of D_3 symmetry since such a distortion allows odd ligand combinations to mix with even metal combinations. Of special importance for this discussion is the fact that the odd $L_\sigma(e_{uc})$ ($c = a, b$) ligand combinations, Table 2, will overlap with the even metal orbitals $M_\pi(e_{gc})$ ($c = a, b$), Scheme 10. We find thus at $q^o + \Delta\phi$ the two ligand-based orbitals of e_u symmetry have the form[29a]:

$$1e_u = L_\sigma(e_{uc})_{(q^o+\Delta\phi)} + \Delta\phi C'_{mix}M_\pi(e_{gc}) \quad (c = a, b) \quad (8)$$

whereas the LUMO for the purpose of this discussion again can be considered unchanged. Here, the mixing coefficient C'_{mix} is the same as in eq 5b in absolute terms. We note however, that it according to perturbation theory[29a] will be of opposite sign as $M_\pi(e_{gc})$ in equation mixes into $L_\sigma(e_{uc})$ "from above", whereas $L_\sigma(e_{uc})$ in eq 5 mixes into $M_\pi(e_{gc})$ from below. Thus, the denominator in eq 5b will have to change sign in the expression for C'_{mix}. Keeping only leading terms affords finally the following relations

Table 3. Calculated Rotatory Strengths for Ligand-to-Metal CT Region for $[Co(en)_n(S\text{-}pn)_{n-3}]^{3+}$ (n = 0, 1, 2, 3)

	real system			
complex	$R(E)^{a,b,e}$	$R(A)^e$	s/h[c]	$\Delta\phi^d$
$\Lambda(\lambda\lambda\lambda)$-(+)-$Co(en)_3$	−45.8	164.3	1.28	− 6.25
$\Delta(\delta\delta\delta)$-(−)-$Co(en)_3$	20.8	−110.6	1.31	4.57
$\Lambda(\delta\delta\delta)$-(+)-$Co(S\text{-}pn)(en)_2$	−87.8	156.4	1.27	−6.73
$\Delta(\delta\lambda\lambda)$-(−)-$Co(S\text{-}pn)(en)_2$	72.0	−112.9	1.29	5.82
$\Lambda(\delta\delta\delta)$-(+)$Co(S\text{-}pn)_2en$	−89.1	165.6	1.27	−6.86
$\Delta(\delta\delta\lambda)$-(−)$Co(R\text{-}pn)_2en$	48.7	−79.1	1.31	4.02
$\Lambda(\delta\delta\delta)$-(+)-$Co(S\text{-}pn)_3$	−85.1	152.8	1.27	−7.20
$\Delta(\delta\delta\delta)$-(−)-$Co(R\text{-}pn)_3$	45.0	−105.7	1.33	4.32

[a] Rotatory strengths in 10^{-40} cgs units. [b] Sum over two E components. [c] Polar ratio, see Scheme 3. [d] Deviation of azimuthal angle from the "octahedral" value of 60°, see Scheme 9. [e] Lowest ligand-to-metal CT region.

(54) McCaffery, A. J.; Mason, S. F. *Mol. Phys.* **1963**, *6*, 359−371.

$$R(A_2) \propto -\Delta\phi C_{mix}\langle L_\sigma(e_{ua})_{(q^o+\Delta\phi)}|\vec{P}|L_\sigma(e_{gb})_{(q^o)}\rangle \times \langle M_\sigma(e_{gb})|\vec{M}|M_\pi(e_{ga})\rangle \quad (9a)$$

$$R(E) \propto -\Delta\phi C_{mix}\langle L_\sigma(e_{ua})_{(q^o+\Delta\phi)}|\vec{P}|L_\sigma(e_{ga})_{(q^o)}\rangle \times \langle M_\sigma(e_{gb})|\vec{M}|M_\pi(e_{ga})\rangle \quad (9b)$$

where we have used $C'_{mix} = -C_{mix}$.

Again the degree of "magnetic intensity" gained will for a given n be larger for the Λ-configuration than the Δ-configuration since $|\Delta\phi^{\Lambda}|$ as explained is larger than $|\Delta\phi^{\Delta}|$, Table 3. It is thus understandable that the rotatory strengths for the first CT bands in absolute terms are larger for the Λ-configuration than the Δ-configuration for a given n, Table 3.

It follows from our analysis that the key CD band in the d−d transition region as well as the first intense ligand to metal CT CD bands for tris-diamine Co(III) complexes owe their intensity to the same mixing of the metal-based t_{2g} orbital and the ligand-based t_{1u} orbital. Our simple theory put forward to interpret the qualitative results would further predict, see eqs 6 and 9, that $R(A_2)$ on the one side and $R(E)$ on the other should be numerically the same for the two types of transitions. This prediction is only born out qualitatively. On the other hand, the simple theory predicts correctly that $R(A_2)$ and $R(E)$ changes sign in going from the d−d region to the CT region, eqs 6 and 9. That the major electrical intensity comes from elements of the type $\langle M_\sigma(e_{uc})|\vec{M}|M_\pi(e_{gc})\rangle$ ($c = a, b$) was also confirmed by an analysis based on eq 2.

The CD Spectra of the *lel*$_3$-Isomer, $\Delta(\lambda\lambda\lambda)$-(−)-[Rh(R-pn)$_3$]$^{3+}$, the *ob*-Isomer, $\Lambda(\lambda\lambda\lambda)$-(+)-[Rh(S-pn)$_3$]$^{3+}$. Figure 4 displays the absorption and CD spectra of the *lel*$_3$-system, Δ-($\lambda\lambda\lambda$)-(−)-[Rh(R-pn)$_3$]$^{3+}$ and the *ob*$_3$-stereoisomer, $\Lambda(\lambda\lambda\lambda)$-(+)-[Rh(R-pn)$_3$]$^{3+}$ obtained from TD-DFT and experimental data.[31] The spectra due to the *lel*$_3$- and *ob*$_3$-stereoisomers afford a weak pair of CD transitions in the range from 32 to 35 × 10^3 cm^{-1}. These CD signals are again due to the same d-to-d HOMO−LUMO singlet excitations at the metal center discussed previ-

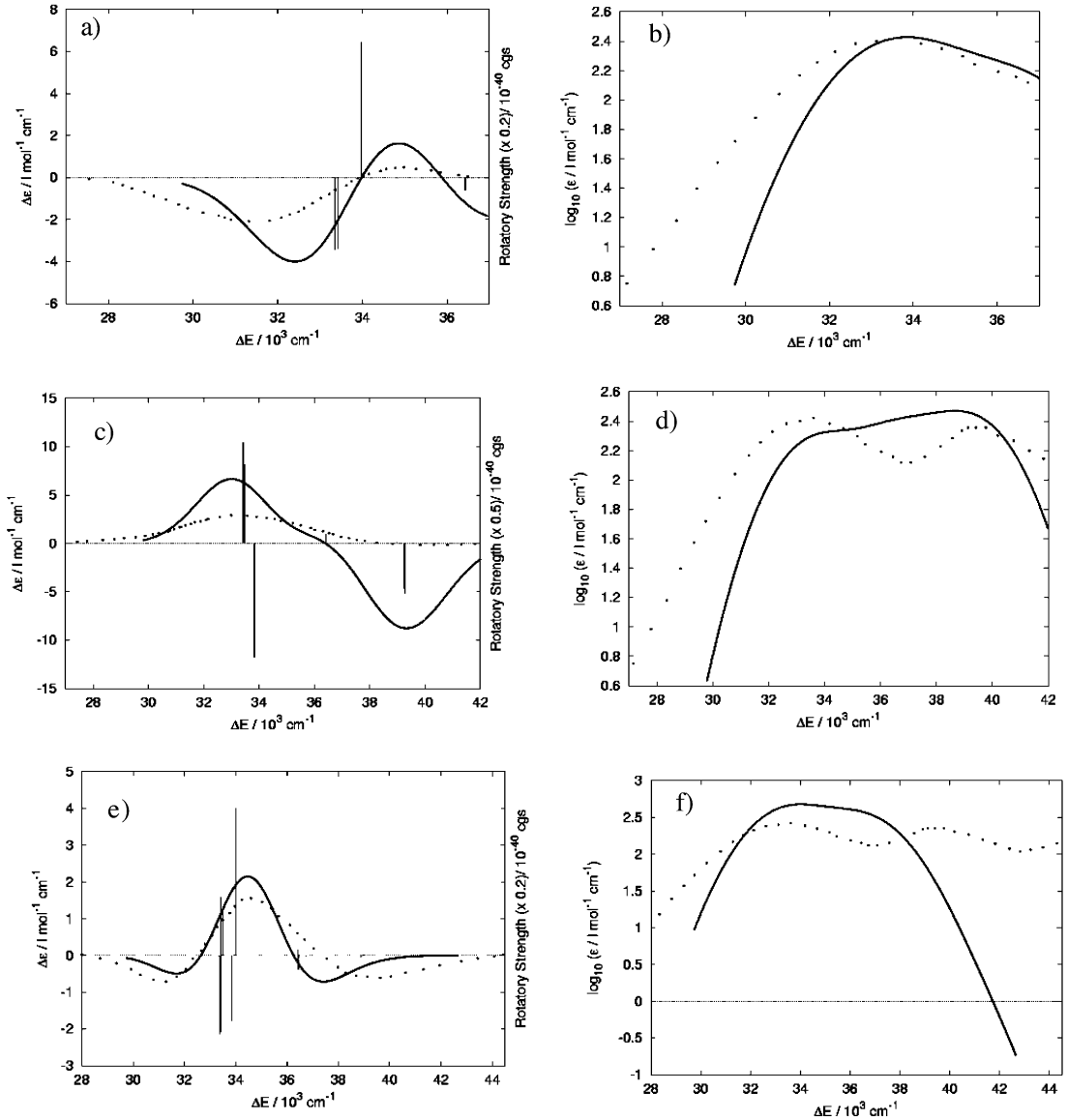

Figure 4. Experimental and simulated absorption spectra (right side graphs) and CD spectra (left side graphs) of (a) and (b): the *lel*$_3$-isomer, Δ-($\lambda\lambda\lambda$)-(+)-[R(pn)$_3$]$^{3+}$; (c) and (d): the *ob*$_3$-isomer, Λ -($\lambda\lambda\lambda$)-(−)-[Rh(R-pn)$_3$]$^{3+}$, and (e) and (f) the mixture of the isomers. Excitation energies and rotatory strengths are plotted as vertical bars. Experiment is dotted lines and theory is solid lines.

ously for the cobalt complexes. They correspond to the symmetry-forbidden $^1T_{1g}$ excitation in O_h and are observed as a pair of ^1E and ^1A transitions in the C_3 symmetric distorted system. The *lel*$_3$-isomer has a theoretical and experimental CD spectra consisting of a major negative and a minor positive CD band (Figure 4a), similar to the two CD bands arising from the corresponding transition of the *lel*$_3$ Λ-[Co(S-pn)$_3$]$^{3+}$-isomer (Figure 1e). The *ob*-isomer gives a single major positive CD band, resembling the CD band associated with the corresponding transition of *ob* Δ-[Co(S-pn)$_3$]$^{3+}$-isomer (Figure 2e). The CD spectra of the mixture of isomers (Figure 4c) formed in the reaction between propylenediamine and rhodium trichloride, when compared with the corresponding experimental spectra of the individual *lel*- and *ob*-isomers, indicate that the mixture consists of 62% of the *lel*$_3$ and 38% of the *ob*$_3$-isomer. Multiplying the TD-DFT rotatory strengths of the *lel*$_3$- and *ob*$_3$-isomers respectively by 0.62 and 0.38 and then adding them, one obtains a curve very similar to the experimental one (see Figure 4e). These results for the Rh(III) complexes show again[26] that the BP86 functional used here works very well for 4d metal complexes, even without any energy shift of the excitation energies.

Conclusions

We have presented TD-DFT calculations on the CD spectra of Λ(*δδδ*)-(+)-[Co(S-pn)$_n$(en)$_{3-n}$]$^{3+}$ (n = 1, 2, 3) and Λ(*δδδ*)-(+)-[Co(en)$_3$]$^{3+}$ as well as the stereoisomers Δ-((*δ*)$_n$(*λ*)$_{3-n}$)-(−)-[Co(S-pn)$_n$(en)$_{3-n}$]$^{3+}$ (n = 1, 2, 3) and Δ(*δδδ*)-(−)-[Co(en)$_3$]$^{3+}$. The low-energy part of the spectra represents HOMO-to-LUMO d-to-d transitions, from t_{2g} to e_g d-based orbitals, Scheme 1. The d−d excitations to $^1E_1$ and $^1A_2$ of $^1T_{1g}$ O_h parentage in the CD spectrum are the most intense as they are magnetically allowed and able to borrow electric intensity from the electrically allowed CT transitions, see Scheme 1. The high-energy part of the recorded CD spectra consist of ligand-to-metal CT transitions from the t_{1u} ligand orbital to the metal-based LUMO e_g , see Scheme 1. Here the ligand-to-metal excitations to $^1E_1$ and $^1A_2$ of $^1T_{1u}$ O_h parentage in the CD spectrum are the most intense as they are electrically allowed, and able to borrow magnetic intensity from d−d transitions, see Scheme 1. The ways by which the d−d transitions borrow electric intensity and the ligand-to-metal transition magnetic intensity are the same. In both cases an azimuthal distortion Δϕ, Schemes 4 and 9, couples the odd $L_\sigma(e_{uc})$ (c = a, b) ligand combinations, Table 2, with the even metal orbitals $M_\pi(e_{gc})$ (c = a, b), Scheme 10. Thus, the electric intensity in the d−d transitions is provided by $L_\sigma(e_{uc})$ (c = a, b) mixing into the d-based HOMOs and the magnetic intensity by $M_\pi(e_{gc})$ (c = a, b) mixing into the t_{1u} ligand orbital.

It follows from both calculations and experiment that the CD spectra in Figure 1 for the Λ-configurations not only differ from the stereoisomers with a Δ-configurations in Figure 2 by a sign for the same n. In addition, the species with a Λ-configurations has larger rotatory strengths in absolute terms than their stereoisomers with a Δ-configurations for both d−d and metal−ligand CT transitions. This difference is explained by observing that $|\Delta\phi^\Lambda| > |\Delta\phi^\Delta|$ as the chelate bite angle of diene chains with a *lel*-conformation is smaller than the chelate bite angle of an *ob*-conformation for Co(III) complexes, Table 1 and Scheme 11. The simplified theory[29a] discussed here is based on the configurational arrangements of the nitrogen atoms around the metal center. It only includes the diene ring to the degree that the ring conformation dictates the geometry of the nitrogens.

Our analysis presented here reveals that there is a close relation between the rotatory strength of the CD bands due to the d−d excitations and the CD bands due to ligand-to-metal CT excitations. Especially, our simple analysis predicts that $R(A_2)$ and $R(E)$ change sign in going from the d−d region to the CT region, eqs 6 and 9, in agreement with experiment. We expect that the simple model presented here can be extended to other metal centers and saturated chelating rings.

Acknowledgment. This work has received financial support from the National Science and Engineering Research Council of Canada (NSERC). One of us (F.E.J.) acknowledges the financial support of CAPES (Brazilian Research Agency). T.Z. thanks the Government of Canada for a Canada Research Chair.

JA047670F